DT#47398 QA:NA

Testing the Concept of Drift Shadow at Yucca Mountain, Nevada

James B. Paces
U.S. Geological Survey
P.O. Box 25046, MS 963
Denver Federal Center
Denver, CO 80225
jbpaces@usgs.gov

Leonid A. Neymark
U.S. Geological Survey
P.O. Box 25046, MS 963
Denver Federal Center
Denver, CO 80225
lneymark@usgs.gov

Teamrat Ghezzehei
Lawrence Berkeley National Laboratory
1 Cyclotron Rd., MS 90R1116
Berkeley, CA 94720
taghezzehei@lbl.gov

Patrick F. Dobson
Lawrence Berkeley National Laboratory
1 Cyclotron Rd., MS 90R1116
Berkeley, CA 94720
pfdobson@lbl.gov

Abstract – *If proven, the concept of drift shadow, a zone of reduced water content and slower ground-water travel time beneath openings in fractured rock of the unsaturated zone, may increase performance of a proposed geologic repository for high-level radioactive waste at Yucca Mountain. To test this concept under natural-flow conditions present in the proposed repository horizon, isotopes within the uranium-series decay chain (uranium-238, uranium-234, and thorium-230, or ^{238}U-^{234}U-^{230}Th) have been analyzed in samples of rock from beneath four naturally occurring lithophysal cavities. All samples show ^{234}U depletion relative to parent ^{238}U, indicating varying degrees of water-rock interaction over the past million years. Variations in $^{234}U/^{238}U$ activity ratios indicate that depletion of ^{234}U relative to ^{238}U can be either smaller or greater in rock beneath cavity floors relative to rock near cavity margins. These results are consistent with the concept of drift shadow and with numerical simulations of meter-scale spherical cavities in fractured tuff. Differences in distribution patterns of $^{234}U/^{238}U$ activity ratios in rock beneath the cavity floors are interpreted to reflect differences in the amount of past seepage into lithophysal cavities, as indicated by the abundance of secondary mineral deposits present on the cavity floors.*

I. INTRODUCTION

Effective waste isolation strategies for the high-level radioactive waste repository proposed in the thick unsaturated zone (UZ) at Yucca Mountain, Nevada (Fig. 1), depend in part on only small amounts of water that would contact waste canisters placed in underground drifts [DOE 2002a, section 1.2; DOE 2002b, section 4.2]. Capillary forces in the fractures and matrix surrounding a drift may prevent ground water percolating through the UZ from seeping into the opening (also called "seepage exclusion") [Philip et al. 1989, Houseworth et al. 2003]. Unless gravity forces can overcome capillary forces at the walls of

the drift, water will remain in the rock mass and be diverted around the drift, locally altering the pattern of UZ flow. As a consequence, the drift may act as a barrier to downward percolation, forming a zone of reduced water content and UZ flow velocity beneath the opening relative to conditions in the adjacent rock mass [Birkolzer et al. 1999; DOE 2002, Section 4.2.8.3.1, Figure 4-117). This concept, called "drift shadow," would benefit natural-barrier performance at Yucca Mountain by reducing seepage and increasing UZ travel times of radionuclides released from waste canisters. This ongoing study was designed to investigate the presence of isotopic and chemical variations that may have developed over the last several hundred thousand years around natural, meter-scale cavities in welded tuffs of the proposed repository horizon. This paper documents progress through the end of 2005.

For this study, radioactive disequilibrium in the natural uranium (U)-series decay chain was relied on to identify elemental and isotopic fractionation generated during water-rock interaction [Chabaux et al. 2003]. In geologic systems that remain closed to mass transfer, isotopes in the ^{238}U-series decay chain attain a state of secular equilibrium, where ^{234}U/^{238}U activity ratios (AR) are equal to unity (1.0). However, alpha (α) decay of ^{238}U may cause direct ejection of the daughter nucleus from the solid, radiation damage at the surface of the solid, and radiation-induced oxidation of daughter ^{234}U [Rosholt et al. 1963, Kigoshi 1971, Gascoyne 1992]. These processes result in U-isotope fractionation due to preferential dissolution of the ^{234}U daughter isotope relative to the parent ^{238}U isotope in the presence of migrating water [Osmond and Cowart 1976 and 1982, Andrews et al. 1982, Tricca et al. 2000, Porcelli and Swarzenski 2003]. Small amounts of water-rock interaction over long periods of time at Yucca Mountain have caused preferential removal of ^{234}U relative to ^{238}U in repository-horizon rocks (^{234}U/^{238}U AR less than 1.0) and enrichment of ^{234}U in the percolating UZ water (^{234}U/^{238}U AR greater than 1.0) [Gascoyne et al. 2002, Paces et al. 2002, Paces and Neymark 2004, Neymark and Paces 2005].

Small differences in water-to-rock mass ratios around lithophysal cavities (voids formed during the emplacement and cooling of the 12.8-million-year-old welded Topopah Spring Tuff) persisting over long periods of time can lead to spatial variations in ^{234}U/^{238}U AR of both rocks and water. The degree of secondary redistribution of ^{234}U and ^{238}U between rocks and water migrating through the UZ depends on a number of physical and chemical factors such as porosity, surface area, water content, flow velocity, weathering rates, U concentrations, and adsorption [Tricca et al. 2000, Porcelli and Swarzenski 2003]. Most of these factors are likely to remain constant over 1-meter (m) spatial scales in welded tuffs at Yucca Mountain, which have high degrees of chemical homogeneity [Peterman and Cloke 2002a, 2002b?]. Therefore, differences in water-to-rock mass ratios in the area surrounding a given lithophysal cavity is the main factor controlling differences in ^{234}U/^{238}U AR observed in whole-rock or water samples. The goal of this study is to evaluate whether variations in ^{234}U/^{238}U AR associated

with four individual lithophysal cavities show systematic spatial variations that are consistent with the concept of seepage exclusion and drift shadow.

II. WORK DESCRIPTION

Large (0.6- to 1.2-m-diameter) lithophysal cavities were selected near the contact between the upper lithophysal and middle nonlithophysal subzones of the Topopah Spring Tuff (Tptpul and Tptpmn, respectively, Buesch et al., 1996) exposed in the Exploratory Studies Facility (ESF) at construction stations ESF 29+79 and 30+18 (2,979 m and 3,018 m from the ESF north portal), and from the lower lithophysal subzone of the Topopah Spring Tuff (Tptpll) exposed in the Enhanced Characterization of the Repository Block (ECRB) Cross Drift at construction stations ECRB 16+15 and 16+17 (1,615 m and 1,617 m from the Cross Drift entrance, Fig. 1). Samples were obtained from tunnel walls on an approximate (~)10- to 20-centimeter (cm) grid spacing beneath cavity floors (Fig. 2) using either 1- or 2-cm-diameter bits in a hand-held percussion drill.

Whole-rock uranium isotope data were obtained from ~0.2-gram (g) samples of pulverized drill cuttings digested using hydrofluoric (HF) and nitric (HNO_3) acids in high-pressure Teflon® vessels. Atomic $^{234}U/^{238}U$ ratios were determined using a Thermo-Finnigan Triton® thermal ionization mass spectrometer equipped with ion-counting capabilities and a retarding potential quadrupole (RPQ) to eliminate background counts on minor isotope peaks from adjacent, large-abundance isotopes. Compositions of international isotope standards (NIST SRM 4321 and IRMM-036) were used to evaluate the accuracy and precision of isotope measurements: replicate analyses measured over the course of the study ($^{234}U/^{235}U$ of 0.0072910±0.12% (2σ, n = 99) for NIST SRM-4321, and $^{232}Th/^{230}Th$ of 321,500±3,000 (2σ, n = 26) for IRMM-036) are within analytical uncertainty of certified values. U and Th blanks (mean values of 50 and 600 picograms, respectively) were routinely measured and used for blank corrections. Atomic ratios were converted to AR using known decay constants [Cheng et al. 2000, Jaffey et al. 1971]. Permil (‰) deviations of $^{234}U/^{238}U$ from secular equilibrium values also are given in delta notation ($\delta^{234}U$) using the equation $\delta^{234}U = (\gamma\text{-}1.0) \times 1000$, where γ is the measured $^{234}U/^{238}U$ AR. Resulting 2-sigma (σ) uncertainties in $^{234}U/^{238}U$ AR for individual analyses range from 0.2 to 0.3 % (2 to 3 ‰) of the measured value. Thorium (Th) isotopes also were measured on samples from selected samples to obtain whole-rock $^{230}Th/^{238}U$ AR so that secondary mobility of U could be evaluated relative to insoluble Th. Replicate analyses of a powdered whole-rock sample from one of the same Topopah Spring lithostratigraphic units resulted in relative precision (2 standard deviations) of 0.73 % for U concentrations

and 0.22 % for $^{234}U/^{238}U$ AR (total of 16 analyses) and 0.88 % for Th concentration and 2.6 % for $^{230}Th/^{238}U$ AR (total of 6 analyses). Replicate analyses (20) of a solution of U ore old enough to be in secular equilibrium [Ludwig et al. 1985] analyzed over the same time period yielded mean and two times standard error values of 0.9984 ±0.0005 $^{234}U/^{238}U$ AR and 1.003 ±0.003 for $^{230}Th/^{238}U$.

The chemical and isotopic compositions of water percolating through fractures and pores also may be impacted by heterogeneous flow around large lithophysal cavities. To test this possibility, ~6-cm-diameter dry-drilled core was obtained from five 6-m-long horizontal boreholes drilled into the Tptpll subzone between construction stations ECRB 16+10 and 16+18. Downhole video logs were used to identify locations of lithophysal cavities intersected by each borehole. Additional boreholes were drilled adjacent to two of the horizontal holes, but at shallow angles (~3-degree plunge) in order to intersect drift-shadow zones 30 to 50 cm below cavity floors exposed in the first boreholes. Water from select core recovered beyond borehole depths of 2 m was extracted by ultra-centrifugation and analyzed for major cations (sodium [Na^+], magnesium [Mg^{2+}], silicon [Si^{4+}], calcium [Ca^{2+}], and potassium [K^+]) and anions (chloride [Cl^-], bicarbonate [HCO_3^-], sulfate [SO_4^{2-}], nitrate [NO_3^-], phosphate [PO_4^{3-}], and bromide [Br^-]) by ion chromatographic methods, for trace elements (lithium [Li], boron [B], strontium [Sr], rubidium [Rb], and U) by inductively coupled plasma quadrupole mass spectrometry, and for $^{234}U/^{238}U$ and $^{87}Sr/^{86}Sr$ by thermal ionization mass spectrometry.

Numerical simulations of UZ fracture flow were conducted to predict the size of drift-shadow zones that would potentially develop beneath meter-scale lithophysal cavities. The analytical solution of Philip et al. [1989], and existing hydrologic property data for the Tptpll [Houseworth et al. 2003], were used for simulations. The model simulates flow in a fracture-matrix continuum with advective and diffusive exchange between the two flow regimes. As a result, a wide range of fracture properties can be simulated, corresponding to observed variations in natural fractures in the welded tuffs. After completing the analytical phase of the study, simulation results will be compared to the distribution of measured $^{234}U/^{238}U$ AR to help calibrate predictive models of seepage into underground openings [Finsterle et al. 2003].

III. RESULTS

III.A. Whole-Rock Analyses

Preliminary results indicate that Yucca Mountain whole-rock samples under the 4 lithophysal cavities have $^{234}U/^{238}U$ AR ranging from 0.922 to 0.998 (Fig. 3A). These data indicate preferential loss of ^{234}U relative to ^{238}U from rock to percolating water over time due to α-recoil processes and variable water-to-rock mass ratios. The degree of ^{234}U depletion varies

systematically between the different sites (Fig. 3A), with the largest ^{234}U depletions present in ESF samples (mean $^{234}U/^{238}U$ AR of 0.934 and 0.939 for ESF 29+79 and ESF 30+18, respectively) and the smallest ^{234}U depletions in samples from ECRB samples (mean $^{234}U/^{238}U$ AR of 0.983 and 0.966 for ECRB 16+15 and ECRB 16+17, respectively). Systematic variations in U concentration also are observed between sites, although substantial overlap is present (Fig. 3A). Contributions of U from construction activities is negligible in tunnel-wall samples, considering the low porosity of the welded tuffs (0.09 to 0.15 cm^3/cm^3) (Rautman and Engstrom, 1996) and the small concentrations of U in construction water derived from supply well UE-25 J-13 (0.5 micrograms per liter [μg/L] with $^{234}U/^{238}U$ AR = 7.2 [Paces et al., 2002]), which is approximately 10^4 times less abundant than U in whole-rock samples.

Combined $^{234}U/^{238}U$ AR and $^{230}Th/^{238}U$ AR data from whole rock samples (Fig. 3B) plot near the $^{234}U/^{230}Th$ equiline (loci of points with equal ^{234}U and ^{230}Th activities). These results indicate that ^{234}U mobility has been slow enough to maintain local radioactive equilibrium with daughter ^{230}Th. Similar relations are present in whole-rock data from UZ and shallow saturated zone (SZ) rocks beneath the proposed repository horizon (Calico Hills Formation and Prow Pass Tuff) that span a much wider range in $^{234}U/^{238}U$ AR (open circles in Fig. 3B; data from Neymark et al., this volume). Whole-rock $^{234}U/^{238}U$ AR greater than 1.0 for zeolitized nonwelded tuffs are attributed to sorption of U from percolating UZ water containing elevated $^{234}U/^{238}U$ AR [Neymark et al., this volume].

In addition to differences in mean $^{234}U/^{238}U$ AR between sites, spatial patterns of ^{234}U depletion are present at each site (Fig. 4). For the ~80-cm-wide cavity at ECRB 16+15 (Fig. 4C), samples showing the least amount of ^{234}U depletion are located beneath the cavity floor ($\delta^{234}U$ values ranging from -15 to -2.3 ‰; equivalent to $^{234}U/^{238}U$ AR of 0.985 to 0.998), whereas samples near cavity margins show the greatest amount of ^{234}U depletion ($\delta^{234}U$ values from -23 to -39 ‰; $^{234}U/^{238}U$ AR of 0.977 to 0.961). The opposite distribution of U isotopes is observed for the largest (~130 cm) cavity at ESF 30+18 (Fig. 4B), where samples near cavity margins have $\delta^{234}U$ values of -46 to -63‰ ($^{234}U/^{238}U$ AR of 0.954 to 0.937) and samples beneath the cavity floor have $\delta^{234}U$ values of -58 to -70 ‰ ($^{234}U/^{238}U$ AR of 0.942 to 0.930). Variations in $\delta^{234}U$ are less pronounced for the ~60-cm-wide cavity at ESF 29+79 (Fig. 4A), which has the greatest overall degree of ^{234}U depletion of the four cavities analyzed. However, samples with less ^{234}U depletion are present beneath the cavity including a single sample with a $\delta^{234}U$ value much closer to secular equilibrium (-17‰, reproduced on two separate aliquots). Variations in $\delta^{234}U$ for samples from the ~60-cm-wide cavity at ECRB 16+17 (Fig. 4D) also are less systematic than patterns observed for larger cavities.

III.B. Pore-Water Analyses

Drilling activities were completed in October 2005, and pore-water extractions were obtained for several intervals of core from a borehole at ECRB station 16+16. Rock porosity and volumetric water contents reported for samples from the Tptpll subzone in a nearby borehole (USW SD-12 [Rautman and Engstrom 1996, Table G-1]) have median values of 0.098 and 0.083 cm^3/cm^3, respectively, indicating median relative saturations of ~0.85. Initial results for core samples obtained during this study indicate gravimetric moisture contents of 0.029 to 0.049 g water per g rock (approximately equivalent to 0.073 to 0.12 cm^3/cm^3), but may depend more on the degree of core fragmentation than location with respect to lithophysal cavity boundaries. Fragmented core has lower moisture content caused by greater losses during dry-drilling relative to intact core. Samples of pore water from this core are more dilute than pore water samples elsewhere in the UZ (Peterman and Marshall, 2002). Preliminary data for seven pore-water samples have average concentrations and standard deviations of 10±6 milligrams per liter [mg/L] Cl^- and 12±6 mg/L SO_4^{2-} compared to values of 47±30 Cl^- and 56±36 mg/L SO_4^{2-} for 58 pore-water samples from densely welded Topopah Spring Tuff reported by Peterman and Oliver [2006]. Uranium concentrations in pore water samples in this study range from 1 to 5 μg/L.

III.C. Numerical Modeling

Numerical modeling focused on simulating drift-shadow dimensions for theoretical matrix- and fracture-flow systems (Fig. 5). The dual permeability flow model used to simulate flow and transport around an underground drift [Houseworth et al. 2003] was scaled to dimensions appropriate for the meter-size lithophysal cavities investigated during this study. Preliminary modeling results indicate that a drift shadow is not likely to develop under conditions dominated by matrix flow. However, simulations indicate that small drift shadows should form under the gravity-dominated advective fracture-flow regime present within the proposed repository horizon. Under these conditions, drift shadows are not predicted to develop beneath cavities much less than 1-m in diameter; however, shadow zones should be observable beneath larger cavities. The length of the shadow zone (L_β in Fig. 5) is related to the rock hydraulic properties and the cavity radius (R). Using a wide variety of hydraulic properties (fine sand, sandstone, fractured tuff), shadow zone lengths beneath a 1-m-diameter spherical cavity are estimated to be less than 10 cm but between 60 and 90 cm beneath a 2-m-diameter cavity. Current models do not address conditions where percolation fluxes exceed the seepage threshold and water accumulates on cavity floors.

IV. DISCUSSION AND CONCLUSIONS

Preliminary results indicate that all whole-rock samples are depleted in ^{234}U relative to parent ^{238}U. These data are consistent with previous results for samples of Topopah Spring Tuff at Yucca Mountain [Gascoyne et al. 2002, Paces et al. 2002, Paces and Neymark 2004, Neymark and Paces 2005]. Variations in observed $^{234}U/^{238}U$ AR indicate that rocks in the proposed repository horizon were subjected to variable water-to-rock mass ratios during the past million years. These data support the use of $^{234}U/^{238}U$ AR as a sensitive indicator of water-rock interaction in rock that otherwise exhibits remarkable degrees of geochemical homogeneity [Peterman and Cloke 2002]. Radioactive equilibrium between ^{234}U and ^{230}Th (Fig. 3B) indicates that bulk leaching of more soluble U relative to less soluble Th is very low in this environment, otherwise $^{230}Th/^{238}U$ AR values would be higher due to U loss and data would plot to the right of the equiline.. Nevertheless, some secondary mobility of U is likely. Preliminary X-ray fluorescence analyses of these whole-rock samples indicate that the systematic differences in U concentrations observed between lithophysal-cavity sites (Fig. 3A) are not the result of differences in primary magmatic compositions. Samples of Tptpmn rock at ESF 29+79 and ESF 30+18 near Drill Hole Wash have lower U concentrations and lower $^{234}U/^{238}U$ AR values relative to the samples of Tptpll rock at ECRB 16+15 and ECRB 16+17 in the central part of the proposed repository block (Fig. 1). Therefore, the positive correlation between U concentrations and $^{234}U/^{238}U$ AR for these samples (Fig. 3A) are consistent with greater long-term losses of both ^{238}U and ^{234}U from the rock as a consequence of higher water-to-rock mass ratios in different areas of the proposed repository block.

Other factors besides time-integrated water fluxes may influence differences in $^{234}U/^{238}U$ disequilibrium between the different sample sites. Most notably, differences in the effective surface areas from which recoil isotopes are lost play an important role in determining overall degrees of ^{234}U depletion. Direct measurements of effective surface area were not made on samples during this study. However, only small, statistically insignificant differences in rock porosity are observed between the mean value of 0.081 $\pm$0.025 cm^3/cm^3 (2σ) for Tptpmn rock (36 samples) and 0.107 $\pm$0.061 cm^3/cm^3 (2σ) for Tptpll rock (42 samples) from nearby borehole USW SD-12 [Rautman and Engstrom, 1996, Table G-1]. Therefore, both the U concentration and $^{234}U/^{238}U$ AR data shown in Fig. 3A tentatively are interpreted as an indication of greater time-integrated water fluxes in the upper part of the Tptpmn near the north bend of the ESF (cavities at ESF 29+79 and 30+18), compared to fluxes in the stratigraphically lower Tptpll in the central part of the proposed repository block (cavities at ECRB 16+15 and 16+17). Mineral line surveys in the tunnels indicating greater abundances of secondary minerals in fractures and lithophysal cavities in the vicinity of the ESF north bend relative to other areas in the ESF and ECRB (James B. Paces, USGS, written commun., 1998; Brian D. Marshall, USGS, unpub. data, 2005) are consistent with data in Fig. 3A, implying higher overall water fluxes around cavities at ESF stations 29+79 and 30+18.

Patterns of $^{234}U/^{238}U$ variation at individual sample sites imply that the long-term distribution of water flow around cavities is heterogeneous. Whole-rock samples beneath the cavity at ECRB 16+15, and possibly at ESF 29+79 and ECRB 16+17, are less depleted in ^{234}U relative to samples near cavity margins. These results indicate that the rock mass beneath these cavities had lower water-to-rock mass ratios, supporting the concept that seepage was excluded more effectively from these cavities relative to the cavity at ESF 30+18. A well-defined drift shadow appears to have developed at the larger ECRB 16+15 cavity as predicted by numerical simulations. The numerical model also predicts that drift shadows are likely to be less apparent at the ESF 29+79 and ECRB 16+17 cavities because of their smaller size (~60 cm). In contrast, the pattern of $^{234}U/^{238}U$ variation associated with the large cavity at ESF 30+18 implies the presence of greater amounts of water seepage into this cavity, resulting in accumulation of flow along the floor of the cavity and greater amounts of water-rock interaction in the underlying rock.

Evidence for past seepage into cavities is indicated by secondary-mineral deposits (primarily calcite and opal) present on cavity floors. Mineral deposits are substantially thicker and more widespread on the floor of the cavity at ESF 30+18 (up to 3 cm thick) compared to sparse deposits in cavities at ECRB 16+15 and ECRB 16+17 (less than 0.5 cm thick) and ESF 29+79 (less than 1 cm thick). Greater amounts of mineral deposits at ESF 30+18 are interpreted as greater solute supply to the floor of this cavity by fluid flux compared to the other cavities. Therefore, greater amounts of seepage flux at ESF 30+18 are likely to have overwhelmed any drift-shadow effects caused by capillary forces at cavity walls.

Preliminary results support the concepts of seepage exclusion and drift shadow in cavities where percolation fluxes do not exceed seepage thresholds. The extent and applicability of these concepts is being tested further on additional tunnel-wall rock samples and pore water extracted from new drillcore as part of this ongoing study.

ACKNOWLEDGMENTS

This work was done by the U.S. Geological Survey in cooperation with the U.S. Department of Energy under Interagency Agreement Number DE-AI28-02RW12167, funded through the U.S. Department of Energy's Office of Science and Technology & International program. Any use of trade, product, or firm names used in this report is for descriptive purposes only and does not imply endorsement by the U.S. Geological Survey. Analytical support from Loretta Kwak, Kevin Scofield, Thomas Oliver, and Brian Marshall is greatly appreciated. Zell Peterman, Andrew Hunt, and Katherine Maher provided comprehensive technical reviews of this paper.

REFERENCES

(ANS-style citation numbering will be incorporated into final submission)

J.N. ANDREWS, I.S. GILES, R.L.F. KAY, D.J. LEE, J.K. OSMOND, J.B. COWART, P. FRITZ, J.F. BARKER, and J. GALE, "Radioelements, Radiogenic Helium and Age Relationships for Groundwaters from the Granites at Stripa, Sweden," *Geochim. Cosmochim. Acta* **46**, 1533 (1982).

BSC (BECHTEL SAIC COMPANY, LLC), "Seepage Calibration Model and Seepage Testing Data," MDL-NBS-HS-000004 REV03, Accession number DOC.20040922.0008, Bechtel SAIC Company, LLC, Las Vegas, Nevada, 246 p. (2004) http://www.ocrwm.doe.gov/documents/amr/41505_osti/index.htm (accessed February 27, 2006).

J. BIRKOLZER, G. LI, C.F. TSANG, AND Y. TSANG, "Modeling Studies and Analysis of Seepage into Drifts at Yucca Mountain," *Jour. Contam. Hydrol.* **38**, 349 (1999).

R.H. BROOKS and A.T. COREY, "Hydraulic Properties of Porous Media," Hydrology Paper No. 3, Civil Engineering Dept., University of Colorado, Fort Collins, Colorado (1964).

D.C. BUESCH, R.W. SPENGLER, T.C. MOYER, and J.K. GESLIN, "Proposed stratigraphic nomenclature and macroscopic identification of lithostratigraphic units of the Paintbrush Group exposed at Yucca Mountain, Nevada," *U.S. Geological Survey Open-File Report* **94-469**, 45 p. (1996)

F. CHABAUX, J. RIOTTE, and O. DEQUINCEY, "U-Th-Ra Fractionation during Weathering and River Transport," *Rev. Mineral. Geochem.* **52**, 533 (2003).

H. CHENG, R.L. EDWARDS, J. HOFF, C.D. GALLUP, D.A. RICHARDS, and Y. ASMEROM, "The Half-Lives of Uranium-234 and Thorium-230," *Chem. Geol.* **169**, 17 (2000).

W.C. DAY, R.P. DICKERSON, C.J. POTTER, D.S. SWEETKIND, C.A. SAN JUAN, R.M. DRAKE II, and C.J. FRIDRICH, "Bedrock geologic map of the Yucca Mountain Area, Nye County, Nevada," *U.S. Geological Survey Geologic Investigations Series* **I-2627**, 21 p., 1 plate (1998)

DOE (U.S. DEPARTMENT OF ENERGY), "Yucca Mountain Preliminary Site Suitability Evaluation," DOE/RW-0549, Accession number MOL.20011101.0082, section 1.2, 466 p., U.S. Department of Energy, Office of Civilian Radioactive Waste Management, Washington, DC (2002a) http://www.ocrwm.doe.gov/documents/sse_a/index.htm (accessed February 27, 2006).

DOE (U.S. DEPARTMENT OF ENERGY), "Yucca Mountain Science and Engineering Report," DOE/RW-0539-1, Accession number MOL.20020404.0042, section 4.2, 942 p., U.S. Department of Energy, Office of Civilian Radioactive Waste Management, Washington, DC (2002b) http://www.ocrwm.doe.gov/documents/ser_b/index.htm (accessed February 27, 2006).

S. FINSTERLE, C.F. AHLERS, R.C. TRAUTZ, and P.J. COOK, "Inverse and Predictive Modeling of Seepage into Underground Openings," *Jour. Contaminant Hydrology* **62-63**, 89 (2003).

M. GASCOYNE, "Geochemistry of the Actinides and Their Daughters," *in* Uranium-Series Disequilibrium: Applications to Earth, Marine, and Environmental Sciences (2nd ed.), M. Ivanovich, and R.S. Harmon (eds.), p. 34, Clarendon Press, Oxford, U.K. (1992).

M. GASCOYNE, N.H. MILLER, and L.A. NEYMARK, "Uranium-Series Disequilibrium in Tuffs from Yucca Mountain, Nevada, as Evidence of Pore-Fluid Flow Over the Last Million Years," *Appl. Geochem.* **17**, 781 (2002).

J.E. HOUSEWORTH, S. FINSTERLE, and G.S. BODVARSSON, "Flow and Transport in the Drift Shadow in a Dual-Continuum Model," *Jour. Contaminant Hydrology*, **62-63**, 133 (2003).

A.H. JAFFEY, K.F. FLYNN, L.E. GLENDENIN, W.C. BENTLEY, and A.M. ESSLING, "Precision Measurements of Half-Lives and Specific Activities of ^{235}U and ^{238}U," *Phys. Rev.* **C.4**, 1889 (1971).

K. KIGOSHI, "Alpha-Recoil Thorium-234: Dissolution into Water and the Uranium-234/Uranium-238 Disequilibrium in Nature," *Science* **173**, 47 (1971).

K.R. LUDWIG, A.R. WALLACE, and K.R. SIMMONS, "The Schwartzwalder Uranium Deposit, II: Age of Uranium Mineralization and Pb-Isotope Constraints on Genesis," *Econ. Geol.* **80**, 1858 (1985).

G.S. MONGANO, W.L. SINGLETON, T.C. MOYER, S.C. BEASON, G.L.W. EATMAN, A.L. ALBIN, and R.C. LUNG, "Geology of the ECRB Cross Drift – Exploratory Studies Facility, Yucca Mountain Project, Yucca Mountain, Nevada," *Bureau of Reclamation and U.S. Geological Survey Milestone* **SPG42GM3**, Denver, CO (1999). http://www.ocrwm.doe.gov/documents/spg42gm3_a/index.htm (accessed February 27, 2006)

L.A. NEYMARK, and J.B. PACES, "Unsaturated-Zone Water/Rock Interaction and U-Series Isotope Mobility at Yucca Mountain, Nevada," *Geochim. Cosmochim. Acta, Special Supplement* **69**, A478 (2005).

L.A. NEYMARK, J.B. PACES, D.T. VANIMAN, and S.J. CHIPERA, "Uranium-Series Constraints on Subrepository Water Flow at Yucca Mountain," *Proc. Eleventh Int'l High-Level Radioactive Waste Management Conference, Las Vegas, Nevada, April 30–May 4, 2006*, American Nuclear Society, La Grange Park, Illinois (2006, this volume).

J.K. OSMOND and J.B. COWART, "The Theory and Uses of Natural Uranium Isotopic Variations in Hydrology," *Atomic Energy Rev.* **14**, 621 (1976).

J.K. OSMOND and J.B. COWART, "Ground Water," *in* Uranium-Series Disequilibrium—Applications to Environmental Problems (1st ed.), M. Ivanovich and R.S. Harmon (eds.), p. 202-245, Clarendon Press, Oxford, U.K. (1982).

J.B. PACES, K.R. LUDWIG, Z.E. PETERMAN, and L.A. NEYMARK, "$^{234}U/^{238}U$ Evidence for Local Recharge and Patterns of Ground-Water Flow in the Vicinity of Yucca Mountain, Nevada, USA," *Appl. Geochem.* **17**, 751 (2002).

J.B. PACES and L.A. NEYMARK, "U-Series Isotopes as Indicators of Water/Rock Interaction in the Unsaturated Zone at Yucca Mountain, Nevada, USA," *in* R.B. Wanty and R.R. Seal, II (eds.), *Proc. of Eleventh Int'l Symposium on Water-Rock Interaction, June 27–July 2, 2004, Saratoga Springs, New York*, p. 475-479, A.A. Balkema Publishers, Leiden, The Netherlands (2004).

Z.E. PETERMAN and P.L. CLOKE, "Geochemistry of Rock Units at the Potential Repository Level, Yucca Mountain, Nevada," *Appl. Geochem.* **17**, 683; and erratum, 955 (2002).

Z.E. PETERMAN and B.D. MARSHALL, "Geochemistry of Pore Water from Densely Welded Topopah Spring Tuff at Yucca Mountain, Nevada," *Geol. Soc. America Abst. Prog.* **34**, 308 (2002).

Z.E. PETERMAN and T.A. OLIVER, "Geochemistry of Natural Components of the Near-Field Environment, Yucca Mountain, Nevada," *Proc. Eleventh Int'l High-Level Radioactive Waste Management Conference, Las Vegas, Nevada, April 30–May 4, 2006*, American Nuclear Society, La Grange Park, Illinois (2006, this volume).

J.R. PHILIP, J.H. KNIGHT, and R.T. WAECHTER, "Unsaturated Seepage and Subterranean Holes: Conspectus, and Exclusion Problem for Cylindrical Cavities," *Water Resources Research* **25**, 16 (1989).

D. PORCELLI and P.W. SWARZENSKI, "The Behavior of U- and Th-Series Nuclides in Ground Water," *Rev. Mineral. Geochem.* **52**, 317 (2003).

C.A. RAUTMAN and D.A. ENGSTROM, "Geology of the USW SD-12 Drill Hole, Yucca Mountain, Nevada," SAND96-1368, Accession number MOL.19970613.0101, 131 p., Sandia National Laboratories, Albuquerque, New Mexico (1996). Accessed January 31, 2006, at http://www.lsnnet.gov (LSN# DEN000864830).

J.N. ROSHOLT, W.R. SHIELDS, and E.L. GARNER, "Isotopic Fractionation of Uranium in Sandstone," *Science* **139**, 224 (1963).

A. TRICCA, D. PORCELLI, and G.J. WASSERBURG, *Factors Controlling the Groundwater Transport of U, Th, Ra, and Rn, Proc. Indian Acad. Sci.: Earth Planet. Sci.*, Vol. 109, No. 1, p. 95, Indian Academy of Sciences, Bangalore, India (2000).

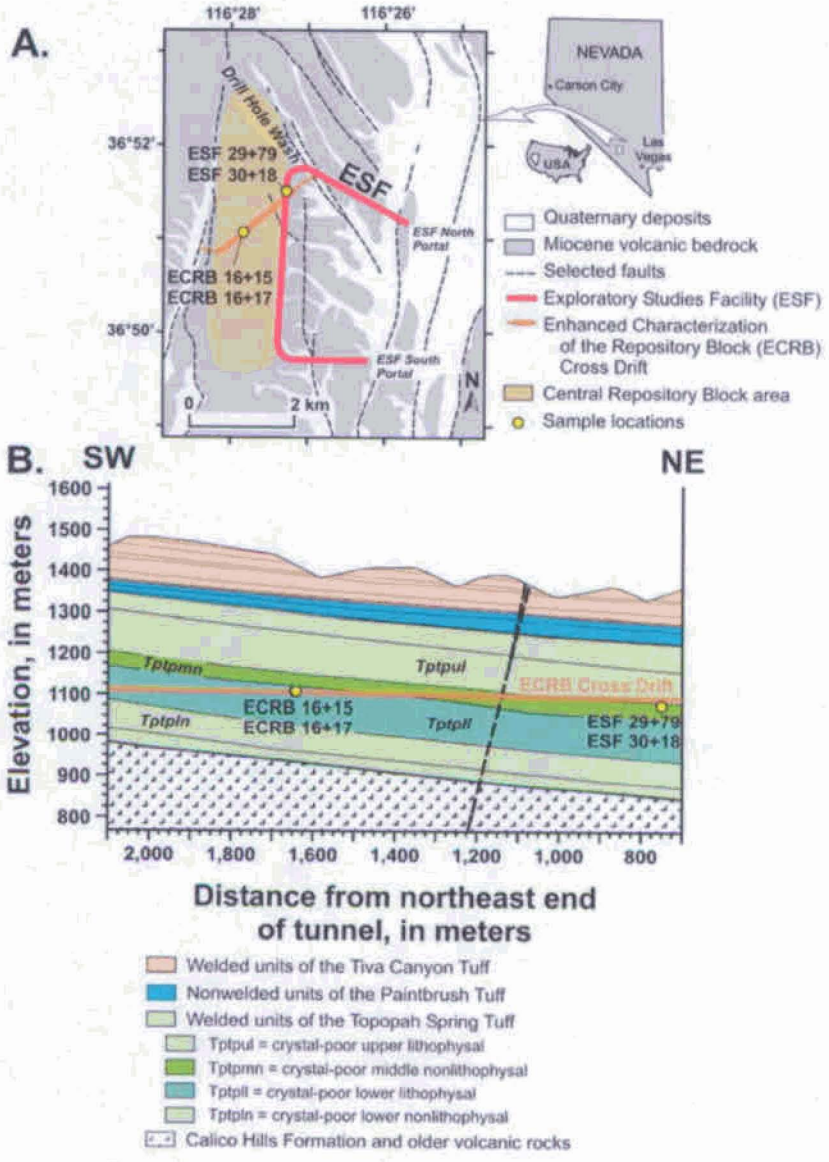

Fig. 1. (A) Schematic map showing the distribution of Miocene bedrock and Quaternary surface deposits at Yucca Mountain, Nevada, along with traces of selected faults, locations of the Exploratory Study Facility (ESF) tunnel and Enhanced Characterization of the Repository Block (ECRB) Cross Drift, and locations of samples collected from tunnel walls (modified from DOE 2002b, Figure 1-14 with geology modified from Day et al., Figure 3). (B) Cross section along the trace of the ECRB Cross Drift (thick orange line in A) showing generalized lithostratigraphy and sample locations (geology from Mongano et al., 1999; Topopah Spring subzone designations from Buesch et al., 1996).

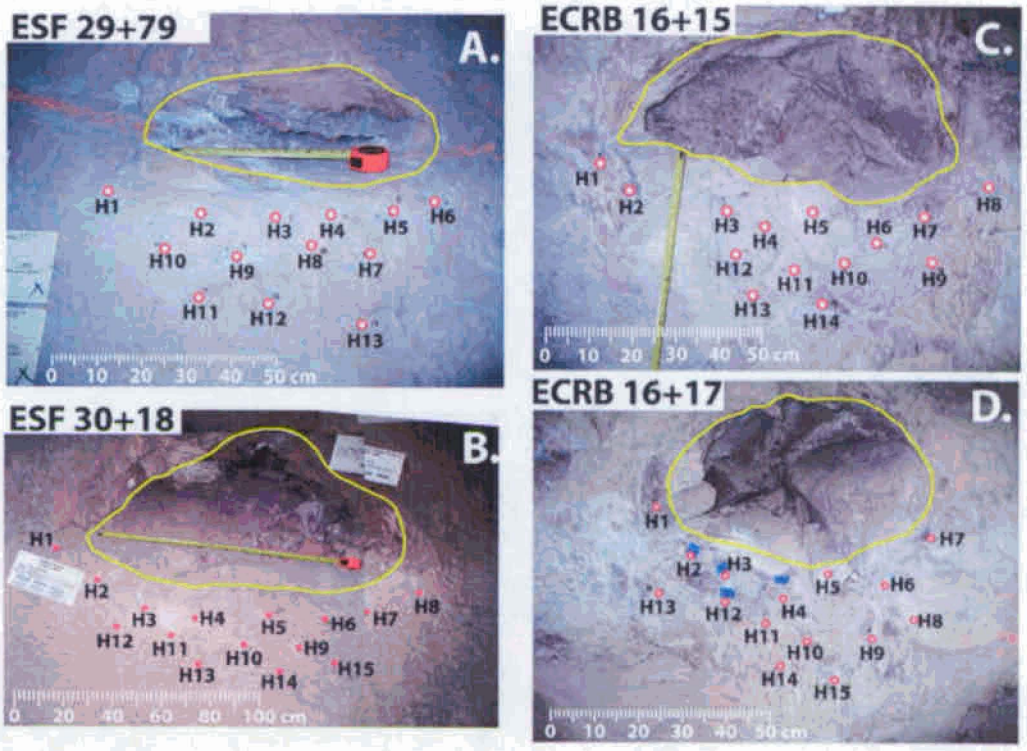

Fig. 2. Photographs of lithophysal cavities exposed in tunnel walls. Cavities are outlined in yellow and sample locations are shown as red circles.

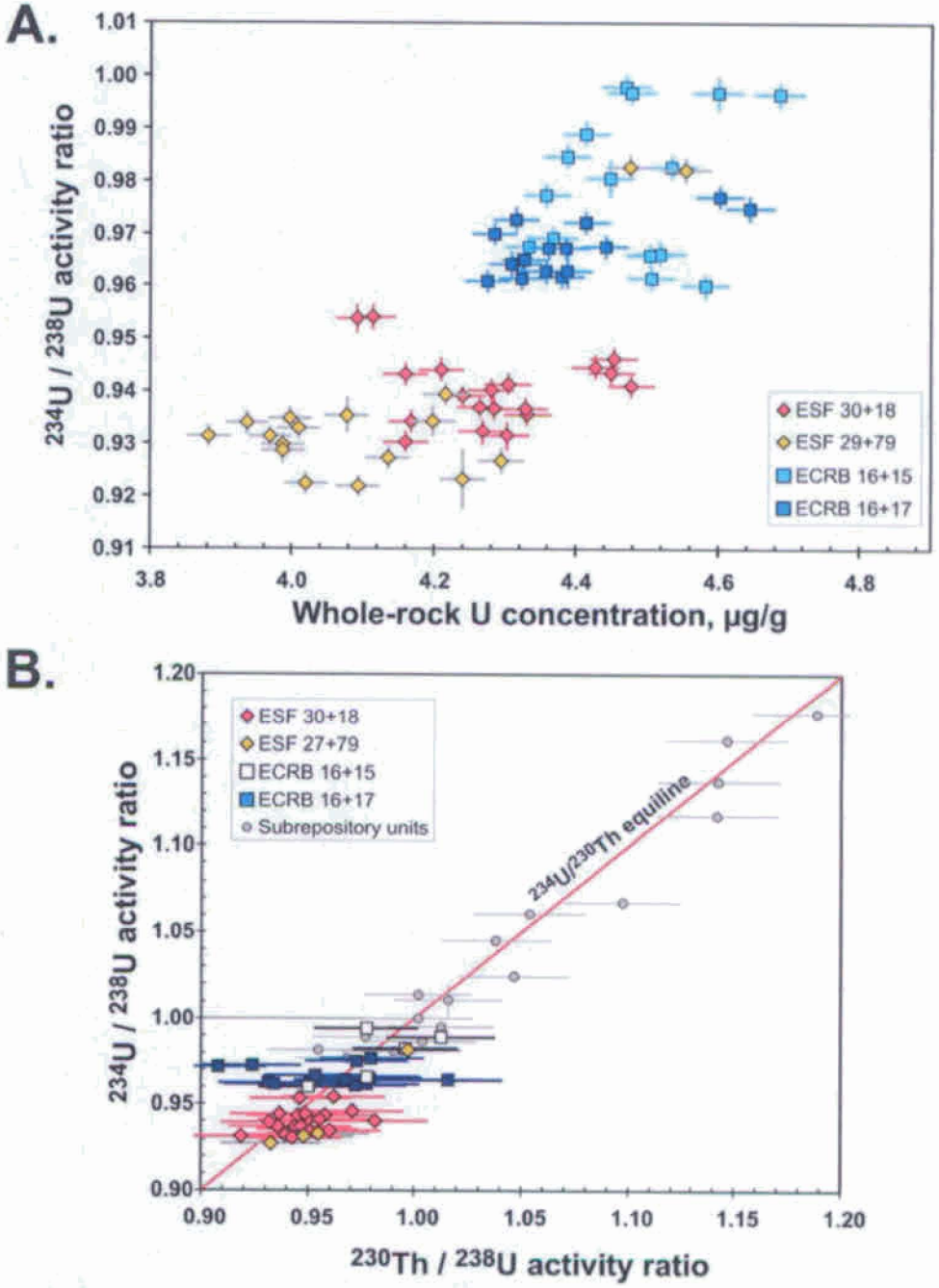

Fig. 3. (A) Relations between uranium (U) concentration and $^{234}U/^{238}U$ activity ratios (AR) for whole-rock samples associated with four lithophysal cavities. Error bars represent 2 sigma (σ) analytical uncertainties. (B) Relations between $^{234}U/^{238}U$ and available $^{230}Th/^{238}U$ AR for whole-rock samples shown in A. Whole-rock data from units beneath the proposed repository horizon (Calico Hills Formation and Prow Pass Tuff; Neymark et al., this volume) are shown for comparison.

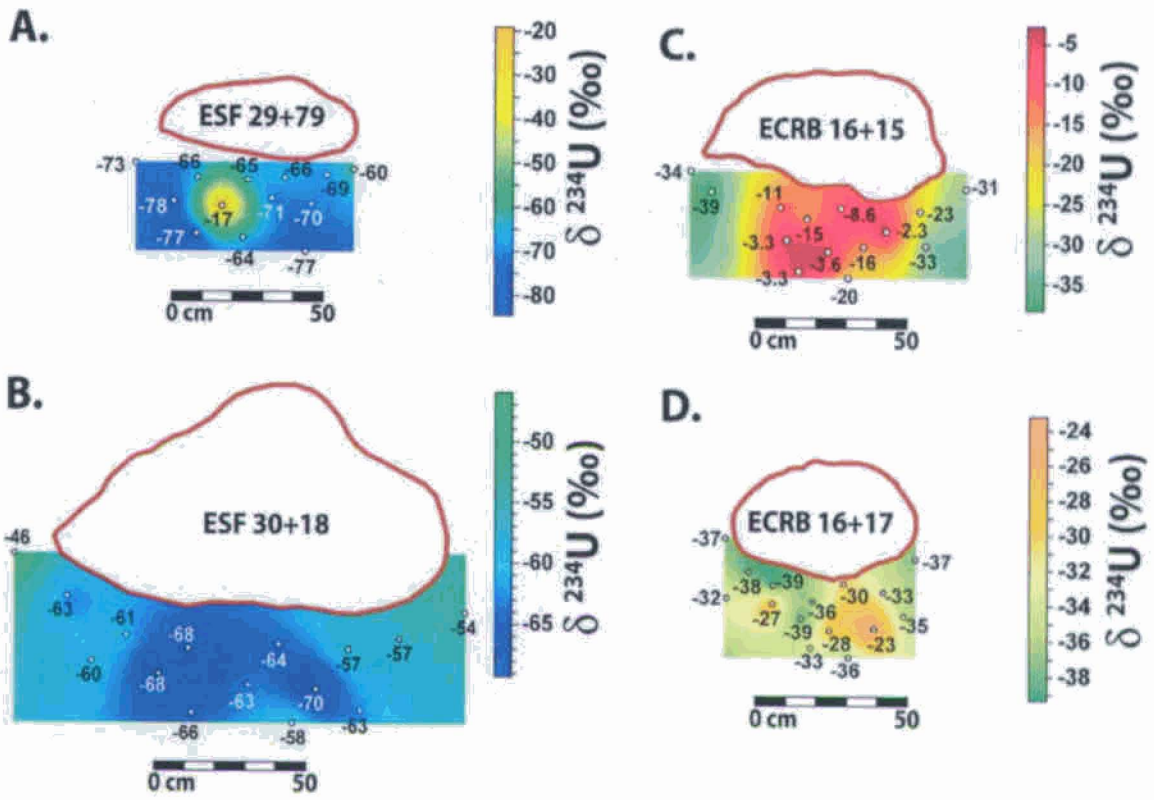

Fig. 4. Preliminary whole-rock $^{234}U/^{238}U$ activity ratios (AR) for lithophysal cavities shown in permil (‰) deviations ($\delta^{234}U$) from secular equilibrium. Analytical uncertainties are range from 2 to 3 ‰ (2 sigma [σ]).

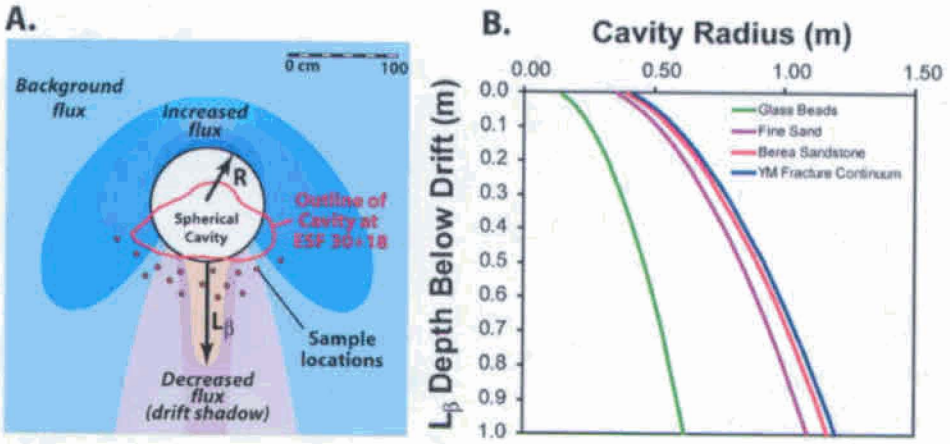

Fig. 5. (A) Conceptual representation of numerical simulations of fracture-continuum flow (colored zones) around a hypothetical spherical cavity (colored zones), showing areas of increased and decreased flux with respect to background flux in undisturbed rock. Also shown is the outline of a lithophysal cavity with sample locations. (B) Results of numerical simulations showing relation between depth of drift shadow (L_β) and cavity radius (R) for materials with different hydraulic properties. Hydrologic properties of glass beads, fine sand, and Berea sandstone were derived from Brooks and Corey (1964); properties of Yucca Mountain fracture continuum were obtained from BSC (2004).